

# Classification with Scattering Operators

Joan Bruna and Stéphane Mallat  
*CMAP, Ecole Polytechnique*  
*91128, Palaiseau Cedex, France*

May 30, 2019

## Abstract

A scattering transform defines a signal representation which is invariant to translations and Lipschitz continuous relatively to deformations. It is implemented with a non-linear convolution network that iterates over wavelet and modulus operators. Lipschitz continuity locally linearizes deformations. Complex classes of signals and textures can be modeled with low-dimensional affine spaces, computed with a PCA in the scattering domain. Classification is performed with a penalized model selection. State of the art results are obtained for handwritten digit recognition over small training sets, and for texture classification.

## 1 Introduction

Affine space models are simple to compute with a Principal Component Analysis (PCA) but are not appropriate to approximate signal classes that include complex forms of variability. Image classes are often invariant to rigid transformations such as translations or rotations, and include elastic deformations, which define highly non-linear manifolds. Textures may also be realizations of strongly non-Gaussian processes that cannot be discriminated with linear models either.

Kernel methods define distances  $d(f, g) = \|\Phi(f) - \Phi(g)\|$ , with operators  $\Phi$  which address these issues by mapping  $f$  and  $g$  into a space of much higher dimension. However, invariance properties and learning requirements

on small training sets, rather suggest to implement a dimensionality reduction.

If  $\Phi$  has appropriate invariants and linearizes small deformations then this paper shows that affine spaces become powerful classification models in the transformed domain. Suppose that  $f(x)$  is translated and deformed into  $D_\tau f(x) = f(x - \tau(x))$ . Let  $\|\nabla\tau(x)\|$  be sup matrix norm of the deformation tensor  $\nabla\tau(x)$ . To linearize small deformations, we impose the following Lipschitz regularity condition:

$$\|\Phi(f) - \Phi(D_\tau f)\| \leq C \|f\| \sup_x \|\nabla\tau(x)\|. \quad (1)$$

A small signal deformation yields a metric modification which is bounded by the deformation amplitude. A Fourier transform modulus  $\Phi(f) = |\hat{f}|$  is invariant to translation but does not satisfy (1) because high frequencies are severely modified by small deformations. Existing invariant representations do not seem either to satisfy this property. Localized transforms such as wavelet transforms are stable relatively to local deformations but are not translation invariant.

Scattering operators constructed in [11, 12], are invariant to translations and Lipschitz continuous relatively to local deformations, up to a log term. These scattering operators  $\Phi$  create invariants by representing signal high frequencies with interference coefficients. This paper models complex signal classes with low-dimensional affine spaces in the scattering domain, which are computed with a PCA. The classification is performed by a penalized model selection.

Scattering operators may also be invariant to any compact Lie subgroup of  $GL(\mathbb{R}^2)$ , such as rotations, but we concentrate on translation invariance, which carries the main difficulties and already covers a wide range of classification applications. Section 2 reviews the construction of scattering operators with a cascade of wavelet transforms and modulus operators, which defines a non-linear convolution network [8]. Section 3 shows that learning affine scattering model spaces has a linear complexity in the number of training samples. Section 4 describes state of the art classification results obtained from limited number of training samples in the MNIST hand-written digit database, and for texture classification in the CUREt database. Softwares are available in “[www.cmap.polytechnique.fr/scattering](http://www.cmap.polytechnique.fr/scattering)”.

## 2 Scattering Transforms

In order to build a representation which is Lipschitz continuous to deformations, a scattering transform begins from a wavelet representation. Translation invariance is obtained by progressively mapping high frequency wavelet coefficients to lower frequencies, with modulus operators described in Section 2.1. Scattering operators iterate over wavelet modulus operators. Section 2.2 shows that it defines a translation invariant representation, which is Lipschitz continuous to deformation, up to a log term. A fast computational algorithm is given in Section 2.3.

### 2.1 Wavelet Modulus Propagator

This section explains how to represent signal high frequencies with lower frequency interference terms, computed with a wavelet transform modulus.

A wavelet transform extracts information at different scales and orientations by convolving a signal  $f$  with dilated bandpass wavelets  $\psi_\gamma$  having a spatial orientation angle  $\gamma \in \Gamma$ :

$$W_{j,\gamma}f(x) = f \star \psi_{j,\gamma}(x) \text{ with } \psi_{j,\gamma}(x) = 2^{-2j}\psi_\gamma(2^jx).$$

At the largest scale  $2^J$ , low-frequencies are carried by a lowpass scaling function  $\phi$ :  $A_Jf = f \star \phi_J$ , with  $\phi_J(x) = 2^{-2J}\phi(2^{-J}x)$  and  $\int \phi(x) dx = 1$ . The resulting wavelet representation is

$$\overline{W}_Jf = \{A_Jf, W_{j,\gamma}f\}_{j < J, \gamma \in \Gamma}.$$

The norm of the wavelet operator is defined by

$$\|\overline{W}_Jf\|^2 = \|f \star \phi_J\|^2 + \sum_{j < J, \gamma \in \Gamma} \|W_{j,\gamma}f\|^2 \quad (2)$$

with  $\|f\|^2 = \int |f(x)|^2 dx$  and it satisfies

$$(1 - \delta)\|f\|^2 \leq \|\overline{W}_Jf\|^2 \leq \|f\|^2 \quad (3)$$

if and only if for all  $\omega \in \mathbb{R}^2$ ,

$$1 - \delta \leq |\hat{\phi}(2^J\omega)|^2 + \frac{1}{2} \sum_{j < J, \gamma \in \Gamma} \left( |\hat{\psi}_\gamma(2^j\omega)|^2 + |\hat{\psi}_\gamma(-2^j\omega)|^2 \right) \leq 1. \quad (4)$$

We consider families of complex wavelets

$$\psi_\gamma(x) = e^{i\xi_\gamma x} \theta_\gamma(x)$$

where  $\theta_\gamma(x)$  are low-pass envelopes. Separable complex wavelets may be constructed from the analytical part of wavelets defining orthonormal bases [12], in which case  $\delta = 0$  and the wavelet transform is unitary. Oriented Gabor functions are other examples of complex wavelets, obtained with a modulated Gaussian  $\psi(x) = e^{i\xi \cdot x} e^{-|x|^2/(2\sigma^2)}$ , which is rotated with  $R_\gamma$  by an angle  $\pi\gamma/|\Gamma|$ :  $\psi_\gamma(x) = \psi(R_\gamma x)$ . In numerical experiments, we set  $\xi = 3\pi/4$ ,  $\sigma = 1$ ,  $|\Gamma| = 6$ , and  $\phi$  is also a Gaussian with  $\sigma = 2/3$ . It satisfies (4) only over a finite range of scales.

If  $f_\tau(x) = f(x - \tau)$  then

$$W_{j,\gamma} f_\tau(x) = W_{j,\gamma} f(x - \tau) \approx W_{j,\gamma} f(x)$$

if and only if  $|\tau| \ll 2^j$ , because  $W_{j,\gamma} f$  has derivatives of amplitude proportional to  $2^{-j}$ . High frequencies corresponding to fine scales are thus highly sensitive to translations.

Translation invariance is improved by mapping high frequencies to lower frequencies with a complex modulus operator. Since  $\psi_\gamma(x) = e^{i\xi_\gamma x} \theta_\gamma(x)$ , we verify that

$$W_{j,\gamma} f(x) = e^{i\xi_{j,\gamma} x} (f_{j,\gamma} \star \theta_{j,\gamma}(x)),$$

where  $\xi_{j,\gamma} = 2^{-j} \xi_\gamma$ ,  $\theta_{j,\gamma}(x) = 2^{-2j} \theta_\gamma(2^{-j} x)$  and  $f_{j,\gamma}(x) = e^{i\xi_{j,\gamma} x} f(x)$ . Wavelet coefficients  $W_{j,\gamma} f(x)$  are located at high frequencies because of the  $e^{i\xi_{j,\gamma} x}$  term. These oscillations are removed by a modulus operator

$$|W_{j,\gamma} f| = |f_{j,\gamma} \star \theta_{j,\gamma}(x)|. \quad (5)$$

The energy of  $|W_{j,\gamma} f|$  is now mostly concentrated in the low frequency domain covered by the envelop  $\hat{\theta}_{j,\gamma}(\omega) = \hat{\theta}_\gamma(2^j \omega)$ . It may however also include some high frequencies produced by the modulus singularities where  $f_{j,\gamma} \star \theta_{j,\gamma}(x) = 0$ . Using complex wavelets is important to reduce the number of such singularities and thus concentrate the information at low frequencies.

If  $f(x) = \sum_n a_n \cos(\omega_n x)$  then one can verify that  $|W_{j,\gamma} f(x)| = c_{j,\gamma} + \epsilon_{j,\gamma}(x)$  where  $\epsilon_{j,\gamma}(x)$  is an interference term. It is a combination of the  $\cos(\omega_n - \omega_{n'})x$ , for all  $\omega_n$  and  $\omega_{n'}$  in the support of  $\hat{\psi}_\gamma(2^j \omega)$ . The modulus yields interferences that depend upon frequency intervals, but it loses the exact frequency locations  $\omega_n$  in each octave.

A complex modulus is applied to all wavelet coefficients, but not to the low frequencies  $A_J f$ , which defines a wavelet modulus propagator:

$$\overline{U}_J f = \{A_J f, |W_{j,\gamma} f|\}_{j < J, \gamma \in \Gamma} .$$

Since  $\||a| - |b|\| \leq \|a - b\|$  and the wavelet transform is contractive, it results that

$$\|\overline{U}_J f - \overline{U}_J g\| \leq \|\overline{W}_J f - \overline{W}_J g\| \leq \|f - g\|$$

and  $\|\overline{U}_J f\| = \|f\|$  if  $\delta = 0$  in (3).

## 2.2 Multiple Paths Scattering

A scattering operator iterates on the propagation operator  $\overline{U}_J$  [11], and defines a convolutional network. It is contractive, translation invariant and Lipschitz continuous to deformations, up to a log factor.

A scattering operator is defined along a path  $p = \{(j_n, \gamma_n)\}_{n \leq |p|}$  which is a family of wavelet indices. It computes  $|p|$  wavelet convolutions and modulus along this path:

$$S(p)f = \underbrace{|\cdots|}_{|p|} f \star \psi_{j_1, \gamma_1} \star \psi_{j_2, \gamma_2} \cdots \star \psi_{j_{|p|}, \gamma_{|p|}} ,$$

with  $j_n < J$  and  $\gamma_n \in \Gamma$ . The scattering output at the scale  $2^J$  is

$$S_J(p)f = S(p)f \star \phi_J .$$

One can verify that scattering coefficients for paths of length  $m + 1$  are computed by applying the wavelet modulus propagator  $\overline{U}_J$  to scattering coefficients for all paths  $p$  of length  $|p| = m$ :

$$\{\overline{U}_J S(p)f\}_{p, |p|=m} = \{S_J(p)f\}_{p, |p|=m} \cup \{S(p)f\}_{p, |p|=m+1} . \quad (6)$$

A scattering transform is thus obtained by cascading the propagator  $\overline{U}_J$ , which defines a convolution network illustrated in Figure 1. Computing  $\overline{U}_J f$  generates a first layer of transformed signals  $S(p)f = |f \star \psi_{j,\gamma}|$  for  $p = \{j, \gamma\}$ , and transforms  $f$  into  $S_J(0)f = f \star \phi_J$ . Suppose that all scattered signals  $S(p)f$  have already been computed for  $|p| \leq m$ . According to (6), the next layer  $m + 1$  is calculated by applying  $\overline{U}_J$  to each  $S(p)f$  on the  $m^{\text{th}}$  layer where  $|p| = m$ . It also transforms the  $m^{\text{th}}$  layer of  $S(p)f$  into  $S_J(p)f = S(p)f \star \phi_J$ .

The scattering operator  $S_J(p)f$  is thus computed along all possible paths with a convolutional network. Convolution networks are general computational architectures introduced by LeCun [8], that involve convolutions and non-linear operators. They are usually constructed with deep-learning back-propagation algorithms [5] to learn the filter coefficients. They have been successfully applied to number of recognition tasks [8] and proposed as models for visual perception [3, 15]. In this case, the filters are dilated wavelets which are not learned, and the non-linearities are modulus operators.

As opposed to standard layered neural networks which output the last layer, all nodes of a scattering network output a signal  $S_J(p)f$  which is used for classification. Depending upon  $|p|$ ,  $S_J(p)f$  gives different type of information on  $f$ . For  $|p| = 0$ ,  $S_J(0)f = f \star \phi_J$  averages the signal. For  $|p| = 1$ ,  $S_J(p)f = |f \star \psi_{j_1, \gamma_1}| \star \phi_J$  is an averaged wavelet modulus, which tends to the  $\mathbf{L}^1$  norm of wavelet coefficients when  $J$  increases. For  $|p| \geq 2$ , it provides higher order interferences between the signal components along different orientations and frequency octaves.

For appropriate complex wavelets, one can prove [12] that the energy  $\sum_{|p|=m} \|S_J(p)f\|^2$  of a scattering layer  $m$  tends to zero as  $m$  increases. This decay is fast. Numerically the maximum network depth is typically limited to  $m_0 = 3$ .

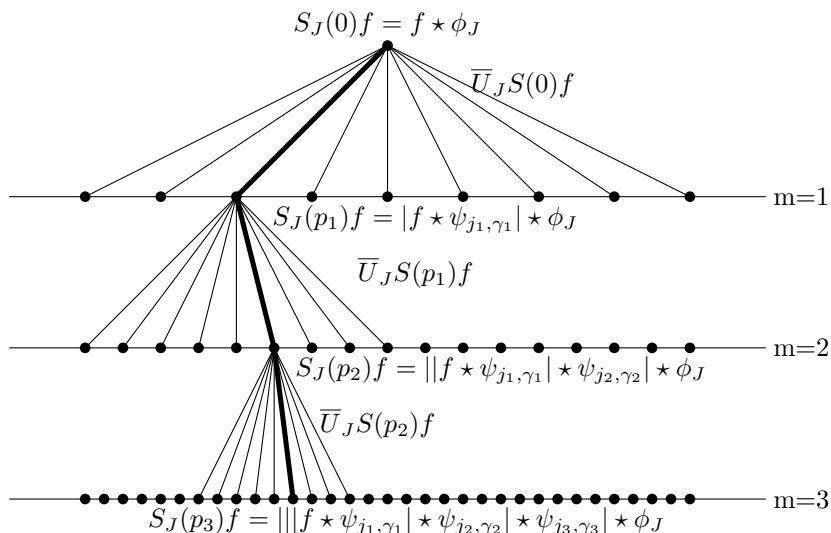


Figure 1: A scattering transform implements a layered convolution network which iterates on a wavelet modulus propagator  $\bar{U}_J$ .

The scattering metric for  $\Phi = S_J$  is obtained with a summation over all paths  $p$ :

$$\|S_J f - S_J g\|^2 = \sum_p \|S_J(p)f - S_J(p)g\|^2 ,$$

where  $\|S_J(p)f\|^2 = \int |S_J(p)f(x)|^2 dx$ . Since  $S_J$  is calculated in (6) by iterating on the contractive propagator  $\bar{U}_J$ , it results that it is also contractive [10]

$$\|S_J f - S_J g\|^2 \leq \|f - g\|^2 .$$

Scattering operators are not only contractive but also preserve the norm. For appropriate complex wavelets which satisfy (4) for  $\delta = 0$ , one can prove [12] that  $\|S_J f\| = \|f\|$ .

When a signal is translated  $f_\tau(x) = f(x - \tau)$ , the scattering transform is also translated

$$S_J(p)f_\tau(x) = S_J(p)f(x - \tau)$$

because it is computed with convolutions and modulus. However, when  $J$  increases,  $S_J(p)f(x)$  tends to a constant because of the convolutions with  $\phi_J$ . It thus becomes translation invariant and one can verify [12] that the asymptotic scattering metric is translation invariant:

$$\lim_{J \rightarrow \infty} \|S_J f - S_J f_\tau\| = 0 .$$

For classification the key scattering property is its Lipschitz continuity to deformations  $D_\tau f(x) = f(x - \tau(x))$ . Let  $|\tau|_\infty = \sup_x |\tau(x)|$  and  $|\nabla\tau|_\infty = \sup_x |\nabla\tau(x)| < 1$ , where  $|\nabla\tau(x)|$  is the matrix sup norm of  $\nabla\tau(x)$ . Along paths of length  $|p| \leq m_0$ , one can prove [12] that for all  $2^J \geq |\tau|_\infty/|\nabla\tau|_\infty$  the scattering metric satisfies

$$\|S_J D_\tau f - S_J f\| \leq C m_0 \|f\| |\nabla\tau|_\infty \log \frac{|\tau|_\infty}{|\nabla\tau|_\infty} . \quad (7)$$

The scattering operator is thus Lipschitz continuous to deformations, up to a log term. It shows that for sufficiently large scales  $2^J$ , the signal translations and deformations are locally linearized by the scattering operator.

### 2.3 Fast Scattering Algorithm

Fast scattering computations are possible because the scattering energy  $\|S_J(p)f\|^2$  is highly concentrated along a small set of paths. A scattering transform is calculated along these paths with an  $O(N)$  algorithm.

Section 2.1 explains that  $|f \star \psi_{j,\gamma}|$  has an energy mostly located over lower frequencies. As a result  $|f \star \psi_{j,\gamma}| \star \psi_{j',\gamma'}$  is negligible if  $j' \leq j$ . The scattering energy is thus concentrated on progressive paths  $p = \{j_n, \gamma_n\}_{n \leq |p|}$  which satisfy  $j_{n+1} > j_n$ . Since  $j_n < J$ , progressive paths have a length  $|p| \leq J$ . Since  $\|S_J(p)f\|$  tends to zero as  $|p|$  increases, progressive paths are computed up to a maximum length  $|p| \leq m_0$ , which is typically 3 in numerical applications. If there are  $|\Gamma|$  different mother wavelets  $\psi_\gamma$  then the number of progressive paths  $p$  of length  $|p| \leq m_0$  is  $O(J^{m_0}|\Gamma|^{m_0})$ .

The scattering transform is implemented along progressive paths for  $|p| \leq m_0$ , by iterating on wavelet transforms and modulus operators, with the layered network illustrated in Figure 1. Each  $S(p)f$  is computed with wavelet convolutions and is sampled at intervals  $\Delta 2^{j_{|p|}}$  where  $2^{j_{|p|}}$  is the scale of the last wavelet on the path. The oversampling factor is typically  $\Delta = 1/2$  to avoid aliasing. The averaged signal  $S_J(p)f(n) = S(p)f \star \phi_J(n)$  is sampled at intervals  $\Delta 2^J$ . The addition of a new element  $(j, \gamma)$  at the end of a path  $p$  is written  $p + (j, \gamma)$ .

---

**Algorithm 1** Progressive scattering calculations

---

```

Set  $S(0)f[n] = f[n]$ ,  $j_{|0|} = 0$ 
for all  $m < m_0$  do
  for all  $p$  with  $|p| = m$  do
    for all  $j > j_{|p|}$  and  $\gamma \in \Gamma$  do
       $S(p + (j, \gamma))f[n] = |S(p)f \star \psi_{j,\gamma}[n\Delta 2^{j-j_{|p|}}]|$ 
    end for
     $S_J(p)f[n] = S(p)f \star \phi_J[n\Delta 2^{J-j_{|p|}}]$ 
  end for
end for
for all  $p$  with  $|p| = m_0$  do
   $S_J(p)f[n] = S(p)f \star \phi_J[n\Delta 2^{J-j_{|p|}}]$ 
end for
Output:  $\{S_J(p)f\}_{|p| \leq m_0}$ 

```

---

One can verify that the scattering signals  $S_J(p)f$  along all progressive paths of length  $|p| \leq m_0$  include  $O(J^{m_0}|\Gamma|^{m_0}N2^{-2J})$  coefficients. The computational cost is driven by the number of operations to compute the subsampled wavelet transform convolutions along  $|\Gamma|$  orientations. With a fast filter bank algorithm, it requires  $O(|\Gamma|N)$  operations for a signal of size  $N$ .

The overall complexity of this algorithm is thus  $O(N4^{-m_0}|\Gamma|^{m_0})$ . Direct convolution calculations with FFTs bring in an extra factor  $\log N$ .

### 3 Classification

Translation invariance and Lipschitz regularity to local deformations linearize small deformations. Signal classes can thus be approximated with low-dimensional affine spaces in the scattering domain. Although the scattering representation is implemented with a potentially deep convolution network, learning is not deep and it is reduced to PCA computations. The classification is implemented with a penalized model selection.

#### 3.1 Affine Scattering Space Models

A signal class  $\mathcal{C}$  can be modeled as a realization of a random process  $F$ . There are multiple sources of variability, due to the reflectivity of the material as in textures, due to deformations or to various illuminations. Illumination variability is often low-frequency and can be approximated in linear spaces of dimension close to 10 [1]. This property remains valid in the scattering domain. A scattering operator also linearizes local deformations and reduces the variance of large classes of stationary processes. One can thus build a linear affine space approximation of  $S_J F$ . A scattering transform  $S_J F$  along progressive paths of length  $|p| \leq m_0$  is a vector of size  $O(N)$ , which may be much smaller than  $N$  if  $J$  is large.

The affine space  $\mathbf{A}_k$  of dimension  $k$  which minimizes the expected projection error  $E\{\|S_J F - P_{\mathbf{A}_k}(S_J F)\|^2\}$  is

$$\mathbf{A}_k = \mu_J + \mathbf{V}_k \tag{8}$$

where  $\mu_J(p, x) = E\{S_J(p)F(x)\}$  and  $\mathbf{V}_k$  is the space generated by the first  $k$  eigenvectors of the covariance operator of  $S_J(p)F(x)$ . The space dimension  $k$  is limited to a maximum value  $K$ .

These affine space models are estimated by computing the empirical average and the empirical covariance of  $S_J(p)f(x)$ , for all training signals  $f \in \mathcal{C}$ . The empirical covariance is diagonalized to estimate the  $K$  eigenvectors of largest eigenvalues. Under mild conditions [17], the sample covariance matrix  $\hat{\Sigma}$  converges in norm to the true covariance when the number of training signals is of the order of the dimensionality of the space where  $S_J F$  belongs.

Dimensionality reduction is thus important to learn affine space models from few training signals.

---

**Algorithm 2** Learning affine models for  $\mathcal{C}$

---

**for** each training signal  $f \in \mathcal{C}$  **do**  
    compute  $S_J f$   
**end for**  
Compute the empirical average  $\hat{\mu}$  and covariance  $\hat{\Sigma}$ .  
Compute with a thin SVD the  $K$  eigenvectors of  $\hat{\Sigma}$  of largest eigenvalues.

---

The computational complexity to estimate affine space models  $\hat{\mathbf{A}}_k$  is dominated by eigenvectors calculations. To compute the first  $K$  eigenvectors, a thin SVD algorithm requires  $O(TKN)$  operations, where  $T$  is the number of training signals.

### 3.2 Linear Model Selection

Let us consider a classification problem with several classes  $\{\mathcal{C}_i\}_{1 \leq i \leq I}$ . We introduce a classification algorithm which selects affine space models by minimizing a penalized approximation error.

Each class  $\mathcal{C}_i$  is represented by a family of embedded affine spaces  $\mathbf{A}_{k,i} = \hat{\mu}_i + \mathbf{V}_{k,i}$ , where  $\mathbf{V}_{k,i}$  is the space generated by the first  $k$  eigenvectors  $\{e_{i,l}\}_{l \leq k}$  of the empirical covariance matrix  $\hat{\Sigma}_i$ . For a fixed dimension  $k$ , a space  $\mathbf{A}_{k,i}$  is discriminative for  $f \in \mathcal{C}_i$  if the projection error of  $S_J f$  in  $\mathbf{A}_{k,i}$  is smaller than its projection in the other spaces  $\mathbf{A}_{k,i'}$ :

$$\forall i' \quad , \quad \|S_J f - P_{\mathbf{A}_{k,i'}}(S_J f)\|^2 \geq \|S_J f - P_{\mathbf{A}_{k,i}}(S_J f)\|^2 \quad ,$$

with

$$\|S_J f - P_{\mathbf{A}_{k,i}}(S_J f)\|^2 = \|S_J f - \hat{\mu}_i\|^2 - \sum_{l=1}^k |\langle S_J f - \hat{\mu}_i, e_{i,l} \rangle|^2 \quad .$$

Model selection for classification is not about finding an accurate approximation model as in model selection for regression but looks for a discriminative model [2]. If  $S_J f$  for  $f \in \mathcal{C}_i$  is close to the class centroid  $\hat{\mu}_i$  then low-dimensional affine spaces  $\mathbf{A}_{k,i}$  are highly discriminative even if the remaining error is not negligible, because it is unlikely that any other low-dimensional affine space  $\mathbf{A}_{k,i'}$  yields a comparable error. If  $f$  is an ‘‘outlier’’

which is far from the centroid  $\hat{\mu}_i$  then a higher dimensional approximation space  $\mathbf{A}_{k,i}$  is needed for discrimination. It is therefore necessary to adjust the dimensionality of the discrimination space to each signal  $f$ . The class index  $i$  of  $f$  is estimated by adjusting the dimension  $k$  of the space  $\mathbf{A}_{k,i}$  that yields the best approximation, with a penalization proportional to the space dimension  $k$  [2]:

$$\hat{i}(f) = \operatorname{argmin}_{i \leq I} \min_{k \leq K} \|S_J f - P_{\mathbf{A}_{k,i}}(S_J f)\|^2 + \beta k .$$

---

**Algorithm 3** Classification of  $f$

---

```

compute  $S_J f$ 
for each class  $\mathcal{C}_i$  do
     $L(i) = \min_{0 \leq k \leq K} \|S_J f - P_{\mathbf{A}_{k,i}}(S_J f)\|^2 + \beta k$ .
end for
 $\hat{i}(f) = \operatorname{argmin}_{i \leq I} L(i)$ 

```

---

The minimum penalized energy  $L(i)$  is computed from the  $K$  inner products of  $S_J f$  with the eigenvectors  $\{e_{i,l}\}_{l \leq K}$  that generate the embedded affine spaces  $\mathbf{A}_{k,i}$  for  $k \leq K$ . The overall computational complexity is thus  $O(KIN)$ .

This classification algorithm depends upon the penalization factor  $\beta$  and the scale  $2^J$  of the scattering transform. These two parameters are optimized with a cross-validation mechanism. It minimizes a classification error computed on a validation subset of the training samples, which does not take part in the affine model learning.

- Increasing the scale  $2^J$  reduces the intra-class variability of the representation by building invariance, but it can also reduce the distance across classes. The optimal size  $2^J$  is thus a trade-off between both.
- The penalization parameter  $\beta$  is similar to a threshold on  $|\langle S_J F - \hat{\mu}_i, e_{i,k} \rangle|^2$ . The model increases the dimension  $k$  of the approximation space if the inner product is above  $\beta$ . Increasing  $\beta$  thus reduces the dimension of the affine model spaces, which is needed when the training sequence is small.

## 4 Classification Results and Analysis

This section presents classification results for handwritten digit recognition, and for texture discrimination with illumination variations. The scattering transform is implemented with the same Gabor wavelets along  $|\Gamma| = 6$  orientations for both problems, and the maximum scattering length is limited to  $m_0 = 2$ .

### 4.1 Handwritten Digit Recognition

The MNIST hand-written digit database provides a good example of classification with important deformations. Table 1 compares scattering classification results for training sets of variable size, with results obtained with deep-learning convolutional networks [14], which currently have the best results. Table 1 compares the PCA model selection algorithm applied on scattering coefficients and an SVM classifier with polynomial kernel whose degree was optimized, also applied on scattering coefficients. Cross validation finds an optimal scattering scale  $J = 3$ , which corresponds to translations and deformations of amplitude about  $2^J = 8$  pixels, which is compatible with observed deformations on digits.

Below  $5 \cdot 10^3$  training examples, a PCA scattering classifier provides state of the art results. It yields smaller errors than deep-learning convolution network which require large training sets to optimize all network parameters with backpropagation algorithms. For  $60 \cdot 10^3$  training samples, the deep-learning convolution network error [6] is below the scattering classifier error. Table 1 shows that applying a linear SVM classifier over the scattering transform degrades the results relatively to a PCA classifier up to large training sets, and it requires much more computations. This is an indirect validation of the linearization properties of the scattering transform.

The last column of Table 1 gives the average dimension  $\bar{k}$  of the best linear approximation spaces  $\mathbf{A}_{k,i}$  selected by the classifier. It mostly increases with the training size because the estimation of high dimensional model spaces requires more training samples. For small training sets, the variance on the PCA eigenvalue estimation is large, which is taken into account by the cross-validation which increases the penalization parameter  $\beta$  to select lower dimensional model spaces.

Figure 2 shows the relative approximation error when approximating a signal class with an affine model in the scattering domain. For digits  $i = 1$

Table 1: Percentage of error as a function of the training size for MNIST. Minimum errors are in bold. The last column gives the average model space dimension  $\bar{k}$ .

Training	ConvNets[14]	Scatt+SVM	Scatt+PCA	$\bar{k}$
300	7.18	21.5	<b>5.93</b>	25
1000	3.21	3.06	<b>2.38</b>	75
2000	2.53	1.87	<b>1.76</b>	130
5000	1.52	1.54	<b>1.27</b>	85
10000	<b>0.85</b>	1.15	1.2	100
20000	<b>0.76</b>	0.92	0.9	130
40000	<b>0.65</b>	0.85	0.86	100
60000	<b>0.53</b>	0.7	0.74	100

and  $i = 4$ , it gives the average Intra-class approximation error of  $S_J F_i$  with a space  $\mathbf{A}_{k,i}$  of the same class, as a function of  $k$ :

$$\text{In}(i) = \frac{E\{\|S_J F_i - P_{\mathbf{A}_{k,i}} S_J F_i\|^2\}}{E\{\|S_J F_i\|^2\}}.$$

It is compared with

$$\text{Out}(i) = \frac{E\{\|S_J F_{i'} - P_{\mathbf{A}_{k,i}} S_J F_{i'}\|^2 \mid i \neq i'\}}{E\{\|S_J F_{i'}\|^2 \mid i \neq i'\}}.$$

which is the average Outer-class approximation error produced by the spaces  $\mathbf{A}_{k,i}$  over all samples  $S_J F_{i'}$  belonging to different classes  $i' \neq i$ . The intra-class error decay is much faster than the outer-class error decay for  $k \leq 10$ , which shows the discrimination ability of low dimensional affine spaces. For  $k \geq 10$ , intra-class versus outer-class distance ratio In/Out is approximatively  $10^{-2}$  and  $10^{-1}$  respectively for the digits  $i = 1$  and  $i = 4$ . It shows the discrimination power of these affine models, and the much larger intra-class variability for hand-written digits 4 than for hand-written digits 1.

The US-Postal Service set is another handwritten digit dataset, with 7291 training samples and 2007 test images  $16 \times 16$  pixels. The state of the art is obtained with tangent distance kernels [4]. Table 2 gives results with a PCA model selection on scattering coefficients and a polynomial kernel SVM classifier applied to scattering coefficients. The scattering scale was also set to  $J = 3$  by cross-validation.

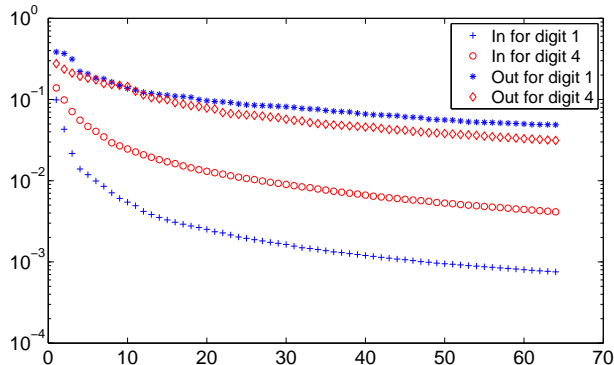


Figure 2: Relative Intra-class In and average Outer-class Out approximation error for the digits  $i = 1$  and  $i = 4$ .

Table 2: Error rate for the whole USPS database.

Scatt+PCA	Scatt+SVM	Tangent kern.[4]	humans
2.64	2.64	<b>2.4</b>	2.37

## 4.2 Texture classification: CUREt

The CureT texture database [9] includes 61 classes of image textures of  $N = 200^2$  pixels, with 46 training samples and 46 testing samples in each class. Each texture class gives images of the same material with different pose and illumination conditions. Specularities, shadowing and surface normal variations make it challenging for classification. Figure 3 illustrates the large intra class variability, and also shows that the variability across classes is not always important.

Classification algorithms with optimized textons have an error rate of 5.35% [9] over this database, and the best result of 2.57% error rate was obtained in [16] with an optimized Markov Random Field model.

Wavelets have been shown to provide useful models for texture analysis [13]. Scattering classification results are shown in table 3, with exactly the same algorithm as for digit classification. With a PCA it greatly improves existing results with an error rate of 0.29%. The SVM classifier with an optimized polynomial kernel on scattering coefficients achieves a larger error

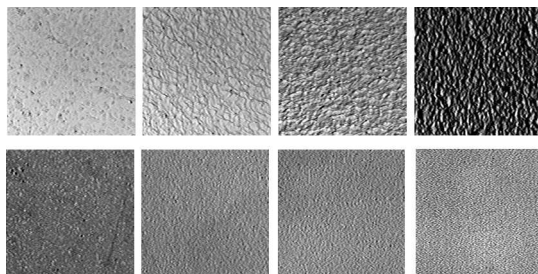


Figure 3: Top row: images of the same texture material with different poses and illuminations. Bottom row: examples of textures that are in different classes despite their similarities.

Table 3: Error rate for the CUREt database

Scatt+PCA	Scatt+SVM	Textons [9]	MRFs [16]
<b>0.29</b>	1.71	5.35	2.57

rate of 1.71%.

CureT textures have a strong variability due to illumination. For a given three-dimensional surface, grey level variability belong to a linear space of dimension of the order of 10 [1], mostly generated by low-dimensional functions when the surface is regular. Textures are not regular three-dimensional surfaces, however scattering operators seem to preserve this low-dimensional approximation capabilities, which may partly explain the large improvements of linear PCA model selections relatively to SVM classifications over scattering coefficients.

Learning adjusts the scattering scale to  $J = 6$  by cross-validation, which is much larger than for hand-written digit recognition. Choosing a large scale is necessary to reduce the variance of scattering estimators. Indeed, for a given illumination and pose, a texture can be modeled as a realization of a stationary process  $F$ . If  $F(x)$  is stationary, since  $S_J(p)F(x)$  is obtained through convolution and modulus operators, it remains stationary. Moreover  $S_J(p)F(x) = S(p)F \star \phi_J(x)$ , so

$$\mu_J(p, x) = E\{S_J(p)F(x)\} = E\{S(p)F(x)\} = \mu(p) ,$$

which does not depend upon  $J$  and  $x$ . The average scattering coefficients  $\mu(p)$  provide descriptors which discriminate stationary processes including

processes having the same Fourier power spectrum. For a large class of processes, a single texture realization has a variance

$$\sigma^2(S_J F) = \sum_p E\{|S_J(p)F(x) - \mu(p)|^2\}$$

which decreases exponentially with  $J$  [12]. Figure 4 shows the exponential decay of  $\sigma^2(S_J F)$  as a function of  $J$ , averaged over several texture classes. All textures  $F$  are normalized with a zero-mean and a unit variance. This exponential variance reduction is due to the scattering averaging by  $\phi_J$  and to the iterated removal of random phase fluctuations by scattering modulus operators. The cross-validation choice of a large  $J$  results from the need to reach a sufficiently small variance  $\sigma^2(S_J F)$  to optimize classification results.

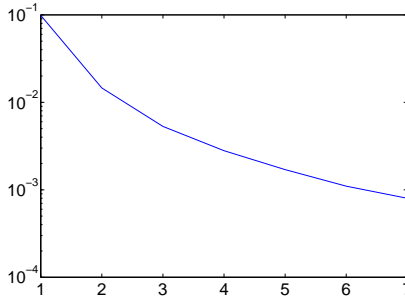


Figure 4: Exponential decay of  $\sigma^2(S_J F)$  in log-scale as a function of  $J$ .

## 5 Conclusion

As a result of their translation invariance and Lipschitz regularity to deformations, scattering operators provide appropriate representations to model complex signal classes with affine spaces calculated with a PCA. Classification with model selection provides state of the art results with limited training size sequences, for handwritten digit recognition and textures. As opposed to discriminative classifiers such as SVM and deep-learning convolution networks, these algorithms learn a model for each class independently from the others, which leads to fast learning algorithms.

For signal classes including large rotations or scaling deformations, it is necessary to use scattering operators which are invariant to these large deformations. This is done with a combined scattering operator which implements

a wavelet transform propagator in space but also along angle parameters to become rotation invariant [12]. Classification of images but also of audio signals is then possible with linear affine space models on combined scattering representations.

## References

- [1] R.Basri, D.Jacobs : “Lambertian Reflectance and Linear Subspaces”, IEEE transactions on Pattern Analysis and Machine Intellingence, feb 2003.
- [2] G. Bouchard and G. Celeux “Selection of generative models in Classification”, IEEE Trans on PAMI,28, 544-554, (2006).
- [3] J. Bouvrie, L. Rosasco, T. Poggio: “On Invariance in Hierarchical Models”. NIPS 2009.
- [4] B.Haasdonk, D.Keysers: “Tangent Distance kernels for support vector machines”, 2002.
- [5] G. Hinton; “Learning to Represent Visual Inputs”; Phil. Trans. R. Soc. B (2010) 365, 177184.
- [6] K. Jarrett, K. Kavukcuoglu, M. Ranzato and Y. LeCun: “What is the Best Multi-Stage Architecture for Object Recognition?”, Proc. International Conference on Computer Vision (ICCV’09), IEEE, 2009.
- [7] F. Lauer, C. Suen, G. Bloch; “A Trainable Feature Extractor for Handwritten Digit Recognition”, Pattern Recognition 40, 6 (2007) 1816-1824.
- [8] Y. LeCun, K. Kavukvuoglu and C. Farabet: “Convolutional Networks and Applications in Vision”, Proc. International Symposium on Circuits and Systems (ISCAS’10), IEEE, 2010
- [9] T. Leung, and J. Malik; “Representing and Recognizing the Visual Appearance of Materials Using Three-Dimensional Textons”. International Journal of Computer Vision, 43(1), 29-44; 2001.
- [10] W. Lohmiller and J.J.E. Slotine “On Contraction Analysis for Nonlinear Systems”, Automatica, 34(6), 1998.

- [11] S. Mallat. “Recursive Interferometric Representation”, Proc. of EUSICO conference, Denmark, August 2010.
- [12] S. Mallat. “Group Invariant Scattering”, CMAP Technical Report, 2010.
- [13] J. Portilla and E P Simoncelli, “A Parametric Texture Model based on Joint Statistics of Complex Wavelet Coefficients”, Int. Journal of Computer Vision, 40(1):49-71, October, 2000
- [14] M. Ranzato, F.Huang, Y.Boreau, Y. LeCun: “Unsupervised Learning of Invariant Feature Hierarchies with Applications to Object Recognition”, CVPR 2007.
- [15] M. Riesenhuber, T. Poggio, “Hierarchical models of object recognition in cortex,” Nature Neuroscience”, 2: 10191025.
- [16] M.Varma, A. Zisserman: “A Statistical Approach To Material Classification Using Image Patch Exemplars”. IEEE Transactions on Pattern Analysis and Machine Intelligence , 31(11):2032–2047, November 2009.
- [17] R.Vershynin: “How close is the sample covariance matrix to the actual covariance matrix?”, Apr 2010